Dynamic range extension of SiPM detectors with the time-gated operation

Eva Vilella[*] and Angel Diéguez

Department of Electronics, Universitat de Barcelona, Martí i Franquès 1, 08028 Barcelona, Spain
[*]*evilella@el.ub.edu*

Abstract: The silicon photomultiplier (SiPM) is a novel detector technology that has undergone a fast development in the last few years, owing to its single-photon resolution and ultra-fast response time. However, the typical high dark count rates of the sensor may prevent the detection of low intensity radiation fluxes. In this article, the time-gated operation with short active periods in the nanosecond range is proposed as a solution to reduce the number of cells fired due to noise and thus increase the dynamic range. The technique is aimed at application fields that function under a trigger command, such as gated fluorescence lifetime imaging microscopy.

References and links

1. S. Donati, *Photodetectors* (Prentice Hall, 1999).
2. A. V. Akindinov, A. N. Martemianov, P. A. Polozov, V. M. Golovin, and E. A. Grigoriev, "New results on MRS APDs," Nucl. Instrum. Methods Phys. Res. Sect. A **387**(1–2), 231–234 (1997).
3. F. Zappa, S. Tisa, A. Tosi, and S. Cova, "Principles and features of single-photon avalanche diode arrays," Sens. Actuators A Phys. **140**(1), 103–112 (2007).
4. S. M. Sze and K. K. Ng, *Physics of Semiconductor Devices* (Wiley-Interscience, 2007), Chap. 2.
5. W. Kucewicz, "Review of ASIC developments for SiPM signal readout," Industria-academy matching event on SiPM and related technologies (CERN, Geneva, Switzerland, 2011).
6. E. Garutti, "Silicon photomultipliers for high energy physics detectors," *arXiv*:1108.3166v1 [physics.ins-det] (2011).
7. M. G. Bagliesi, C. Avanzini, G. Bigongiari, R. Cecchi, M. Y. Kim, P. Maestro, P. S. Marrocchesi, and F. Morsani, "A custom front-end ASIC for the readout and timing of 64 SiPM photosensors," Nucl. Phys. B **215**(1), 344–348 (2011).
8. F. Powolny, E. Auffray, S. E. Brunner, E. Garutti, M. Goettlich, H. Hillemanns, P. Jarron, P. Lecoq, T. Meyer, H. C. Schultz-Coulon, W. Shen, and M. C. S. Williams, "Time-based readout of a silicon photomultiplier (SiPM) for time of flight positron emission tomography (TOF-PET)," IEEE Trans. Nucl. Sci. **58**(3), 597–604 (2011).
9. G. Llosá, P. Barrillon, J. Barrio, M. G. Bisogni, J. Cabello, A. Del Guerra, A. Etxebeste, J. E. Gillam, C. Lacasta, J. F. Oliver, M. Rafecas, C. Solaz, V. Stankova, and C. de La Taille, "High performance detector head for PET and PET/MR with continuous crystals and SiPMs," Nucl. Instrum. Methods Phys. Res. Sect. A **702**, 3–5 (2013).
10. T. Frach, G. Prescher, C. Degenhardt, R. de Gruyter, A. Schmitz, and R. Ballizany, "The digital silicon photomultiplier – Principle of operation and intrinsic detector performance," in *Proceedings of IEEE Nuclear Science Symposium Conference Record* (Orlando, USA, 2009), pp. 1959–1965.
11. T. Frach, G. Prescher, C. Degenhardt, and B. Zwaans, "The digital silicon photomultiplier – System architecture and performance evaluation," in *Proceedings of IEEE Nuclear Science Symposium Conference Record* (Knoxville, USA, 2010), pp. 1722–1727.
12. Thermoelectrically cooled MPPC for photon counting – Active area 1 x 1 mm, Hamamatsu MPPC S11028 series (2013).
13. J. J. Fox, N. Woodard, and G. P. Lafyatis, "Characterization of cooled large-area silicon avalanche photodiodes," Rev. Sci. Instrum. **70**(4), 1951–1956 (1999).
14. B. F. Levine and C. G. Bethea, "Single photon detection at 1.3 μm using a gated avalanche photodiode," Appl. Phys. Lett. **44**(5), 553–555 (1984).
15. M. D. Eisaman, J. Fan, A. Migdall, and S. V. Polyakov, "Invited review article: Single-photon sources and detectors," Rev. Sci. Instrum. **82**(7), 071101 (2011).
16. D. Stoppa, D. Mosconi, L. Pancheri, and L. Gonzo, "Single-photon avalanche diode CMOS sensor for time-resolved fluorescence measurements," IEEE Sens. J. **9**(9), 1084–1090 (2009).
17. Y. Maruyama and E. Charbon, "A time-gated 128x128 CMOS SPAD array for on-hip fluorescence detection," in *Proceedings 2011 International Image Sensor Workshop* (Hookkaido, Japan, 2011), R41.

18. E. Vilella and A. Diéguez, "Readout schemes for low noise single-photon avalanche diodes fabricated in conventional HV-CMOS technologies," Microelectron. J. in press.
19. C. Niclass, "Single-photon image sensors in CMOS: Picosecond resolution for three-dimensional imaging," PhD Thesis Dissertation 4161, École Polytechnique Fédérale de Lausanne (Lausanne, Switzerland, 2008).
20. 1 x 12 VCSEL Array 2.7 – 3.6 Gb/s, 8685–1402, Emcore (2004).

1. Introduction

Traditional silicon photomultiplier (SiPM) detectors [1, 2], also known as multi-pixel photon counters (MPPCs), consist of an array of Geiger-mode Avalanche PhotoDiode (GAPD) cells that are connected in parallel on a common silicon substrate. Each cell is composed of one GAPD sensor [3] in series to a quenching resistor. Due to their GAPD based nature, the principle of operation of SiPMs is therefore the avalanche multiplication [4]. Accordingly, the main features of these devices comprise single-photon and single-particle sensitivity as well as ultra-fast response time, but also a high pattern noise given by dark counts, afterpulses and crosstalks.

So far, two main types of SiPMs have been proposed. In conventional or analog SiPMs, the sensing nodes of all the GAPD cells are connected together. Therefore, the output signal is an analog pulse proportional to the number of fired cells across the array. As a result, the pattern noise at room temperature can range from several hundred kHz/mm^2 to a few MHz/mm^2, which prevents the detection of low intensity radiation fluxes. To extract the information generated by the sensor, conventional SiPMs are typically read out via a multi-channel front-end ASIC, either standard or dedicated [5–9]. In contrast, in digital SiPMs or simply dSiPMs, which are being developed by Philips Digital Photon Counting (PDPC), each GAPD is provided with a modified CMOS readout circuit monolithically integrated on the same substrate [10, 11]. Each cell can be read out individually within the sensing device. Consequently, the frequency of dark counts or dark count rate (DCR) at room temperature of a good GAPD cell can be reduced to a few hundred Hz/photodiode.

In analog and digital SiPMs, the intensity of the impinging signal is obtained by counting the number of cells fired during a certain integration time. Those cells with an unusually high DCR are fired due to noise most of the time and therefore they prevent the detection of extremely weak intensities. Moreover, other cells with a significant pattern noise are gradually fired as the integration time is increased. Consequently, the dynamic range, which is limited by the number of available cells across the detector, is reduced. To solve this problem, analog SiPMs are typically operated at cooled temperatures. In spite of this, the usual pattern noise of these detectors is still of a few kHz/mm^2 at −20 °C [12]. The further decrease of the operating temperature to reduce even more the pattern noise is not an option, since the afterpulsing probability generally increases at low temperatures [13]. In contrast, in the dSiPM developed by PDPC it is possible to switch off by means of the readout circuit those GAPD cells with an abnormally high DCR to reduce the average noise across the detector. According to PDPC, between 5 and 10% of the photodiodes of their arrays with several thousand cells show an abnormally high DCR due to defects. However, the shutdown of these photodiodes is equivalent to the corresponding loss of fill-factor. Consequently, the probability to detect events and the dynamic range are reduced. This situation is not particularly delicate in photon detection applications, where the maximum 30-40% photon detection probability (PDP) of dSiPMs still outperforms the capabilities of many photomultiplier tubes (PMTs), but it is an issue in some HEP applications where having a 100% fill-factor is fundamental. Nevertheless, the situation can also be improved by means of the time-gated operation [14, 15], in which the sensor is periodically switched on and off to reduce the probability to detect the noise counts that interfere with radiation triggered events without losing sensitive area. In this article, the time-gated operation is proposed as an effective method to increase the dynamic range of both analog and digital SiPMs aimed at applications where the signal to be detected originates from a periodic trigger command. Possible application fields that could benefit from this technique are gated fluorescence lifetime imaging microscopy (FLIM) [16, 17], single-photon emission computed tomography

(SPECT) or the high energy physics (HEP) experiments that will take place at the International Linear Collider (ILC).

2. Experimental set-up and proposed technique

The time-gated dSiPM used in this experiment consists of an array of 430 GAPD cells, which are monolithically integrated in the high-voltage austriamicrosystems (HV-AMS) 0.35 μm CMOS process. Each cell consists of a GAPD sensor and a readout circuit. The cell pitch is 22.9 μm x 138.1 μm and the fill-factor of the detector is calculated to be 67%. The cells are biased on one end at a common $V_{BD} + V_{OV}$ and on the other end at a common GNDA, where V_{BD} is the breakdown voltage of the junction, V_{OV} the reverse bias overvoltage to operate the Geiger-mode and GNDA the ground node of the sensor. Additional biases, V_{DD} and V_{SS}, are needed to power the readout electronics. Each readout circuit is composed of 2 MOS switches to activate and deactivate the GAPD according to the time-gated operation, a voltage discriminator to sense the voltage rise at the GAPD anode upon avalanche, a 1-bit memory cell to store the information generated by the GAPD during the gated-on periods and a pass-gate to extract the content of the cell during the gated-off periods. The avalanches are quenched by the parasitic capacitance that the readout circuit induces at the anode of the sensor, which is calculated to be 15.75 fF. A micrograph of the dSiPM detector and the schematic diagram of one GAPD cell are shown in Fig. 1. The MOS switches continuously enable and disable the photodiode by connecting its anode to GNDA and V_{DD}, respectively. Note that V_{OV} is limited to V_{DD}, which is 3.3 V in this technology. The voltage discriminator is based on a simple CMOS inverter, which also digitizes the response of the photodiode. The threshold voltage of the CMOS inverter can be externally adjusted to sense avalanches generated at a low V_{OV}. The memory cell (a pass-gate and a CMOS inverter) is time-gated synchronously with the GAPD, so that the readout circuit samples the response of the photodiode during the gated-on periods and stores the generated value ('0' for no count, '1' for count) during the gated-off periods. The time-gated dSiPM presents a remarkable readout speed, since each cell can be read out in 1.65 ns. Off-cell counters are used to count the avalanches generated during a certain integration time. The detector is mounted on a PCB and connected to a development board (terasIC DE0-Nano with an ALTERA Cyclone IV FPGA), which is used to generate the control signals to operate the detector in the time-gated mode and manage the communication with a PC via a USB. The PC runs a dedicated software developed in C + + that allows to select the duration of the gated-on (t_{on}) and gated-off (t_{off}) periods, as well as the number of times (n_{rep}) that the sequence $t_{on} + t_{off}$ is repeated. The integration time is given by the product of multiplying the gated-on period by the number of repetitions ($t_{on} \cdot n_{rep}$). The PC also displays in real time the number of counts generated by the detector after the integration time.

During the experiment, the time-gated dSiPM was operated with different gated-on periods that range from 200 ns to 3.2 μs, a gated-off period of 1 μs and a reverse bias overvoltage of 1 V. The duration of the gated-off period was chosen to strongly reduce the presence of afterpulses [18], in addition to prevent the data acquisition system from working to the limit. The introduction of a long enough gated-off period suppresses the need for active quenching circuits, which are difficult to implement successfully in monolithically integrated technologies and also area consuming [19]. The number of repetitions was set at $1 \cdot 10^5$ for each of the gated-on periods analyzed to obtain significant statistics. To show the efficiency of the time-gated operation in the reduction of the threshold event of the detector, the time-gated dSiPM was illuminated with a pulsed 850 nm vertical cavity surface-emitting laser (VCSEL) array [20]. The laser was biased at a fixed V_{VCSEL} through a pull-up resistor and pulsed via a fast nFET. The value of V_{VCSEL} ranged between 5.3 and 6 V to generate different optical powers and was increased in steps of 50 mV. The nFET, which was placed between the laser anode and V_{SS}, was periodically switched on and off by means of a control signal generated by the FPGA. The nFET was switched off, and therefore the laser was switched on, during a period of 100 ns within the gated-on period of the detector. Therefore, no counts due to signal were possibly missed. The repetition rate of the laser ranged from 0.24 MHz in the

case of a 3.2 μs t_{on} to 0.83 MHz in the case of a 200 ns t_{on}. The duration of the active window of the laser was adjusted also via software means. The experiment was conducted at room temperature in a black box to protect the detector against uncontrolled light sources. A schematic diagram of the experimental set-up is depicted in Fig. 2. With this experiment, we expected to see that the reduction of the gated-on period decreases the number of cells being fired by the noise, which in turn also maximizes the effective fill-factor and the dynamic range of the detector.
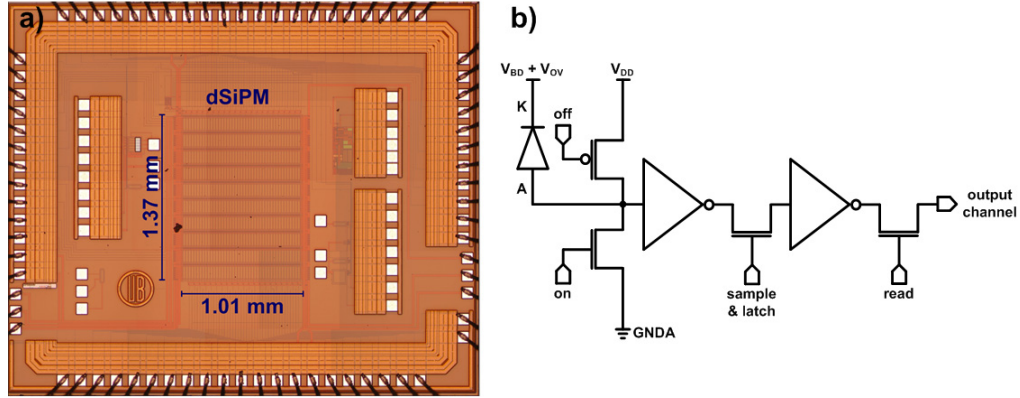

Fig. 1. Micrograph of the dSiPM detector (a) and schematic diagram of one digital GAPD cell (b).
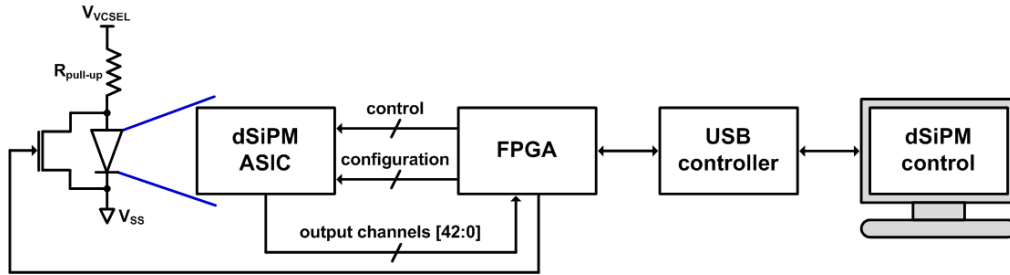

Fig. 2. Schematic diagram of the experimental set-up used to characterize the time-gated dSiPM.

3. Measured results and discussion

To start with, the number of cells fired by the noise during one frame was measured as a function of the gated-on time. For this purpose, the noise counts of all the cells recorded in the dark during the integration time were averaged over all the repetitions:

$$cells\ fired\ by\ noise = \frac{1}{n_{rep}} \sum_{n=0}^{429} noise\ counts_{cell\ n}. \qquad (1)$$

Thus, if all the cells are always silent the result is 0, while if all the cells are always fired the result is 430. The measured results indicate a linear increment, starting from 5.3 fired cells with a gated-on period of 200 ns to 76.6 fired cells with a gated-on period of 3.2 μs (approximately 5 cells more every 200 ns). This result is not biased by the overall efficiency of the detector, which is maximum for gated-on periods longer than 1 ns [18]. Consequently, the effective dynamic range, which is defined as the percentage of available cells with respect to the total number of cells of the detector, is reduced as the gated-on period is increased. The effective dynamic range as a function of the gated-on period is depicted in Fig. 3, where a maximum dynamic range of 98.7% recorded with the 200 ns gated-on period can be

observed. The expected number of fired cells at a particular t_{on} duration can also be obtained from the product of the DCR of the detector by t_{on}:

$$cells\ fired\ by\ noise = DCR \cdot t_{on.} \tag{2}$$

From Eq. (1) and Eq. (2), the expression for calculating the DCR from measured values can be inferred. According to this, the measured DCR of the detector is 25.6 ± 1.06 MHz. Thus, the expected number of fired cells calculated from Eq. (2) is 5.2 ± 0.2 cells fired with a t_{on} of 200 ns, 10.2 ± 0.4 cells fired with a t_{on} of 400 ns and so on until 81.9 ± 3.4 cells fired with a t_{on} of 3.2 µs. As just demonstrated, the number of fired cells also matches well with the experimental results.
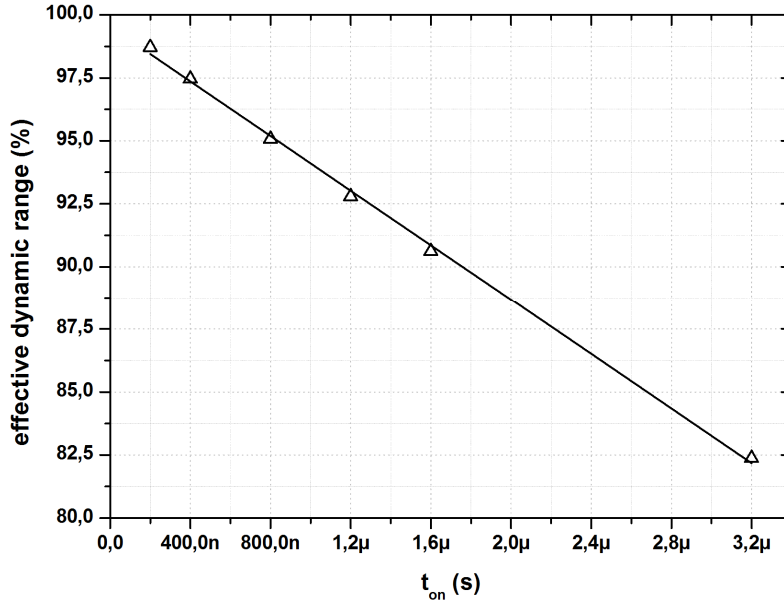

Fig. 3. Effective dynamic range as a function of the gated-on period.

After that, the time-gated dSiPM was illuminated with the pulsed VCSEL array. The number of triggered cells as a function of the optical power received by the sensitive area of the SiPM detector (i.e. optical density expressed in W/SiPM) was investigated for the different gated-on periods 200 ns, 800 ns and 3.2 µs. In this case, the number of cells fired by signal was calculated as:

$$cells\ fired\ by\ signal = \frac{1}{n_{rep}} \sum_{n=0}^{429} counts_{cell\ n} - cells\ fired\ by\ noise, \tag{3}$$

where the term counts includes both noise and signal counts. The measured values, averaged according to Eq. (3), are plotted in Fig. 4. The flat regions of the graph correspond to those optical densities below threshold, where the cells are triggered due to noise only. The threshold optical density is defined as the minimum optical power received by the SiPM from which cells fired by signal can be observed. It is a function of the dynamic range of the detector and therefore of the gated-on period. As the threshold is surpassed, a few cells are fired by the impinging light. Thus, for a gated-on period of 200 ns, an increase in the number of cells fired is sensed from an optical density of 9.46 nW/SiPM. For the gated-on periods of 800 ns and 3.2 µs, the increase is sensed from 9.76 nW/SiPM and 10.07 nW/SiPM, respectively. Also in Fig. 4, it can be observed that the number of cells fired by signal at a particular optical density over the maximum threshold (i.e. over 10.07 nW/SiPM) is approximately the same despite the length of the gated-on period. Thus, when the optical

density is 10.97 nW/SiPM, around 3 cells are fired by signal for all the gated-on periods measured. This result corroborates that the detector is fully efficient during the whole gated-on time. The result obtained is remarkable for low light intensities, which makes the proposed technique especially suitable for low light applications. At high light intensities, the number of cells fired is independent of the t_{on} period, as it should be. Nevertheless, the number of cells fired is low given the reduced PDP of the time-gated dSiPM at the wavelength of the laser (1% at 850 nm). The technique here proposed to reduce the threshold event, which also maximizes the effective fill-factor and the dynamic range of the detector, can be applied to any SiPM, either analog or digital.
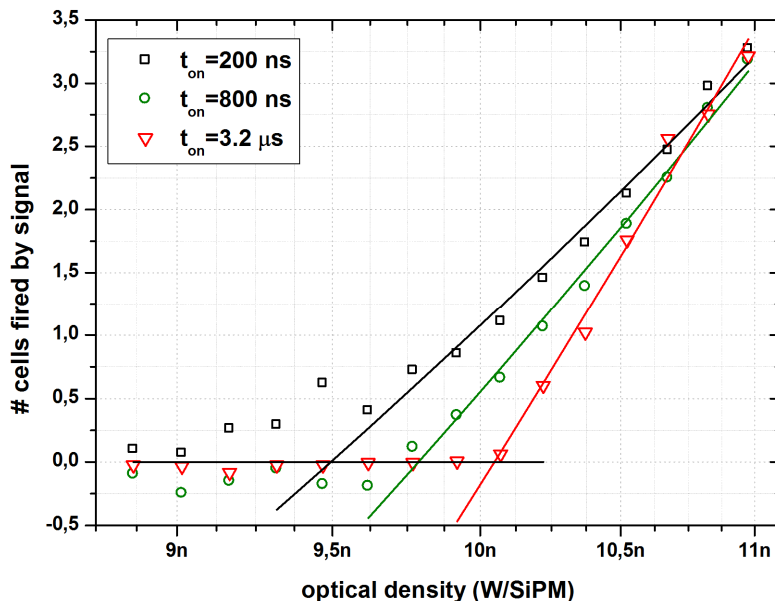

Fig. 4. Number of cells fired by signal as a function of the optical density for different gated-on periods.

4. Conclusion

In this article, a time-gated dSiPM with the readout electronics monolithically integrated on the same substrate of a standard CMOS technology has been presented. The time-gated dSiPM is aimed at application fields that function under a trigger command. It has been demonstrated that the reduction of the gated-on period to some nanoseconds longer than the duration of the expected impinging signal allows to successfully increase the dynamic range of the detector. The experimental characterization at room temperature showed that the number of cells fired by the noise is decreased in 5 fired cells every 200 ns, approximately. Consequently, the dynamic range of the detector is increased. The proposed method can be used by any SiPM detector, either analog or digital.

Acknowledgment